



Changes in targeted metabolomics in lung tissue of chronic obstructive pulmonary disease

Yi Feng^{1#}, Meiqin Xie^{1#}, Qi Liu^{1#}, Jiali Weng¹, Liangyu Wei¹, Kian Fan Chung², Ian M. Adcock², Qing Chang¹, Mengnan Li¹, Yan Huang³, Hai Zhang¹, Feng Li¹

¹Department of Pulmonary and Critical Care Medicine, Shanghai Chest Hospital, Shanghai Jiao Tong University School of Medicine, Shanghai, China; ²Experimental Studies, Airway Disease Section, National Heart and Lung Institute, Imperial College London, London, UK; ³School of Pharmacy, Anhui Medical University, Hefei, China

Contributions: (I) Conception and design: F Li, H Zhang, Y Feng; (II) Administrative support: F Li, H Zhang; (III) Provision of study materials or patients: Y Feng, M Xie, Q Liu, J Weng, L Wei, H Zhang, Q Chang, M Li, Y Huang; (IV) Collection and assembly of data: Y Feng, M Xie, Q Liu, J Weng, L Wei, H Zhang, Q Chang, M Li; (V) Data analysis and interpretation: Y Feng, M Xie, Q Liu; (VI) Manuscript writing: All authors; (VII) Final approval of manuscript: All authors.

[#]These authors contributed equally to the work.

Correspondence to: Feng Li, MD, PhD; Hai Zhang, MD. Department of Pulmonary and Critical Care Medicine, Shanghai Chest Hospital, Shanghai Jiao Tong University School of Medicine, No. 241, West Huaihai Road, Shanghai 200030, China. Email: lifeng741@aliyun.com; zhanghai_241@163.com.

Background: Chronic obstructive pulmonary disease (COPD) is a common chronic lung disease and its incidence is steadily increasing. COPD patients and mouse models of COPD share some similarities in lung pathology and physiology. We performed this study to explore the potential metabolic pathways involved in the pathogenesis of COPD and to discover the COPD-associated biomarkers. Furthermore, we aimed to examine how much the mouse model of COPD was similar and different to human COPD in terms of the altered metabolites and pathways.

Methods: Twenty human lung tissue samples (ten COPD and ten controls) and twelve mice lung tissue samples (six COPD and six controls) were analyzed by targeted HM350 metabolomics, and multivariate and pathway analysis were performed by Kyoto Encyclopedia of Genes and Genomes (KEGG) database.

Results: The counts of many metabolites such as amino acids, carbohydrates and carnitines were changed in both COPD patients and mice compared to controls, respectively. While lipid metabolism was changed only in COPD mice. After KEGG analysis, we found these altered metabolites involved in COPD through aging, apoptosis, oxidative stress and inflammation pathways.

Conclusions: The expressions of metabolites changed in both COPD patients and cigarette smoke exposed (CS-exposed) mice. And there were also some differences between COPD patients and mouse models due to the differences between species. Our study suggested the dysregulation in amino acid metabolism, energy production pathway and perhaps lipid metabolism may be significantly related to the pathogenesis of COPD.

Keywords: Chronic obstructive pulmonary disease (COPD); metabolomics; metabolites; human lung tissue; mouse model

Submitted Dec 01, 2022. Accepted for publication May 12, 2023. Published online May 22, 2023.

doi: 10.21037/jtd-22-1731

View this article at: <https://dx.doi.org/10.21037/jtd-22-1731>

Introduction

Chronic obstructive pulmonary disease (COPD) is a common, preventable and treatable chronic lung disease, with clinical features of persistent airflow limitation and

associated respiratory symptoms, caused by airway and/or alveolar abnormalities due to toxic particles or gases. COPD is still the most prevalent chronic respiratory disease worldwide in 2017, accounting for 55.1% among men and

54.8% among women globally (1), and it is the seventh leading cause of years of life lost around the world (2). The most common cause of COPD is cigarette smoking, but age, genetics and environmental exposures may also play a significant role in the development and progression of COPD (3). Mitochondria are important organelles that are at the center of metabolism and energy generation in the body. Recent studies support the notion that the disorders of metabolism, metabolic pathways and energy homeostasis in mitochondria can result in airway diseases (4), and that these deranged pathways present in COPD can lead to autophagy, apoptosis, inflammation and the ageing process that is at the heart of the pathogenesis of COPD (5).

Currently, the pathogenesis of COPD remains incompletely studied. Metabolomics, as a new detection method for biomarkers, is increasingly used in COPD research of clinical patients and experimental animals (6,7), in order to understand the pathogenesis, phenotypes, diagnosis and interventions (8,9). For example, the pathogenesis of COPD has been explored recently by integrating metabolic and cell signal pathways (10). Metabolomics studies have also reported that changes in metabolites were significantly associated with the presence of COPD (8,11).

Animal models of COPD such as generated by exposure

to cigarette smoke (CS) can help better understand the underlying mechanisms of CS induced COPD and study the role of various inflammatory and metabolic pathways (12,13). Although COPD mouse can mimic some of the features of the disease, this model does not fully reflect all of the characteristic features of human disease due to the physiological, genetic and environmental differences between human and mouse (14). In this study, we examined the changes in metabolites and metabolic pathways in human and mouse lung tissues of COPD using a targeted metabolomics HM350 analysis. We undertook this study in order to explore the potential metabolic pathways involved in the pathogenesis of COPD and to explore the possibility of discovering COPD-associated biomarkers. Furthermore, we wished to examine how much the mouse model of COPD was similar and different to human COPD in terms of the altered metabolic pathways. We present this article in accordance with the ARRIVE reporting checklist (available at <https://jtd.amegroups.com/article/view/10.21037/jtd-22-1731/rc>).

Methods

Study subjects and specimens

Human lung tissues were obtained from ten non-smokers and ten newly-diagnosed COPD patients admitted to Shanghai Chest Hospital for lung cancer surgery between July and August, 2020. The inclusion criteria were as follows: (I) current smokers with a smoking history of ≥ 20 pack-years or non-smokers; (II) aged 39–72 male patients; (III) diagnosed COPD: the diagnosis of COPD was made on the basis of post-bronchodilator $FEV_1/FVC < 70\%$ (FEV_1 : forced expiratory volume in one second; FVC : forced vital capacity) according to the Global Initiative for Chronic Obstructive Lung Disease (GOLD), controls with post-bronchodilator $FEV_1/FVC > 70\%$, and bronchodilation tests were negative in two group patients; (IV) lung cancer stage I or IIA, and no history of chemotherapy or radiation. The following exclusion criteria were used: (I) complicated with respiratory tract infection or other chronic pulmonary diseases (e.g., asthmas, bronchiectasis, interstitial lung diseases, lung fibrosis, pulmonary hypertension, etc.); (II) systemic steroid use within the previous 4 weeks; (III) a history of other cancers, lung cancer stage $> IIA$ or a history of chemotherapy or radiation.

After the lung resection, specimens were dissected at a distance of more than 5 cm from the cancerous tissues

Highlight box

Key findings

- Compared to control, amino acids, carbohydrates and carnitines were changed in both COPD patients and mice, while PUFA metabolism was changed only in COPD mice. Furthermore, we also investigated acylcarnitines metabolism and ferroptosis pathway as overlapping metabolic changes in COPD patients and mice.

What is known and what is new?

- Many studies have determined the metabolic characteristics of COPD in blood and bronchoalveolar lavage fluid.
- We used lung tissue for study, as it can better present the metabolic characteristics of COPD.

What is the implication, and what should change now?

- The altered metabolites involved in COPD through aging, apoptosis, oxidative stress and inflammation, indicating these dysregulations may be related to the development of COPD. Our study may provide potential therapeutic targets for COPD. And due to the differences between humans and mice, the use of COPD mouse model to study diseases has some limitations.

then immediately transferred in liquid nitrogen and stored at -80°C until analysed (15). The study was conducted in accordance with the Declaration of Helsinki (as revised in 2013). This study was approved by the Institutional Ethics Committee of Shanghai Chest Hospital (No. KS1969), and written informed consent was obtained from all subjects.

Mouse model of COPD

Male C57/BL6 mice aged eight to ten weeks were purchased from the Shanghai Super-B & K Laboratory Animal Company (Shanghai, China) and randomly divided into a control group and CS-exposed group with six mice in each group. They were maintained under constant temperature (20°C) and relative humidity (40% to 60%) for twelve hours light and dark cycling with adequate food and water *ad libitum*. Mice were placed into a well-sealed box equipped with measures to prevent lethal asphyxia for CS-exposure (five cigarettes/time, Marlboro Red Label, Longyan Tobacco Industrial Co. Ltd., Fujian, China, with 12 mg tar and 1.0 mg nicotine per cigarette, four times/day, five days/week) for twelve weeks (16,17), while control mice were placed in filtered air only. The individual mouse was considered as an experimental unit in the study.

At the end of 12-week exposure, mice were anesthetized, tracheostomized and placed in a plethysmograph (EMMS, Hants, UK) with a ventilator to measure inspiratory capacity (IC), functional residual capacity (FRC), total lung capacity (TLC), forced vital capacity, forced expiratory volume in first 25 and 50 milliseconds of exhalation (FEV25, FEV50) and chord compliance (Cchord) as previously described (18).

Following terminal anaesthesia, the right lung was removed and stored at -80°C until analysis, while the left lung was inflated with 10% formalin under 25 cm of water pressure for 8 h and then embedded in paraffin. Five μm sections were cut and stained with haematoxylin and eosin (H&E) to determine mean linear intercept (Lm), a measure of interalveolar septal wall distance. Experiments were performed under a project license (No. KS1969) granted by the Institutional Ethics Committee of Shanghai Chest Hospital, in compliance with the institutional laboratory animal management guidelines for the care and use of animals.

Sample process and targeted HM350 metabolomics

Twenty mg of lung tissue samples were crushed, then each sample and standard concentration sample were added with

120 μL working solution, shook at room temperature at 1,200 r/min for 20 min, and then centrifuged at 18,000 g, 4°C for 20 min. After centrifugation, 30 μL of supernatant was transferred to a 96-well plate, and 20 μL of derivatization reagent working solution and N-(3-Dimethylaminopropyl)-N'-ethylcarbodiimide hydrochloride (EDC) working solution were added in turn. Then the 96-well plate was placed in a shaker, 1,200 rpm, 30°C for 60 min; 100 μL of pre-cooled 50% methanol solution was added to each well, and mixed at room temperature at 1,200 rpm for five minutes, then centrifuged at 4,000 g, 4°C for 30 min; 100 μL of the supernatant together with ten μL of the internal standard II working solution were added to a new microplate, mixed at 650 rpm for five minutes and prepared for targeted HM350 metabolomics (BGI-tech, Shenzhen, China).

The liquid chromatography tandem mass spectrometry (LC-MS/MS) scanning mode was Multi Reaction Monitoring (MRM), which has the outstanding advantages of strong specificity, high sensitivity, high accuracy, good reproducibility, wide linear dynamic range and high automated throughput. The analytical instrument for this experiment was LC-MS QTRAP 6500+ (SCIEX, Framingham, MA, USA). The liquid chromatographic parameters and mass spectrometry parameters are chromatographic column: BEH C18 (2.1 mm \times 10 cm, 1.7 μm , Waters Milford, MA, USA) and ion source: Electron Spray Ionization (ESI) +/ESI-, respectively. The integral peak area of the sample metabolite was substituted into the linear equation of the standard curve to calculate the concentration value. The absolute content of metabolites in the actual sample was finally obtained after the concentration value was put into the concentration conversion formula.

Statistical analysis

Data are expressed as the mean \pm standard deviation (SD), and analyzed by Student's *t*-test or Mann-Whitney U test according to the distribution. Correlations were obtained using Pearson or Spearman test. All the analyses were performed using SPSS 22.0. $P < 0.05$ was considered significant.

The multivariate analysis, principal component analysis (PCA), partial least squares-discriminant analysis (PLS-DA), and correlation analysis were performed using R package. PCA was used to show the distribution of the original data. Before establishing PCA model, \log_2 transformation was carried out on the data, and scaling was adjusted using the method of Pareto scaling. PLS-DA was used to

Table 1 Clinical characteristics of subjects

Clinical characteristics	Non-smokers (n=10)	COPD (n=10)	P
Age (years)	55.9±9.79	60.7±6.13	0.205
Sex (male/female)	10/0	10/0	–
Smoking index (pack-years)	0	44.44±14.19	–
BMI, kg/m ²	25.6±3.45	23.90±3.05	0.273
FVC (%pred)	92.57±11.37	78.07±9.29	0.006**
FEV ₁ (%pred)	97.72±10.46	55.38±10.25	<0.001***
FEV ₁ /FVC (%)	81.50±2.60	52.95±8.48	<0.001***
TLC (%pred)	113.14±11.43	142.11±21.69	0.004**
DLCO (%pred)	112.01±166.85	74.71±41.40	<0.001***

Data are presented as mean ± SD. **, P<0.01; ***, P<0.001. BMI, body mass index; FVC (%pred), forced vital capacity percent predicted; FEV₁ (%pred), forced expiratory volume in one second percent predicted; FEV₁, forced expiratory volume in one second; FVC, forced vital capacity; TLC (%pred), total lung capacity percent predicted; DLCO (%pred), diffusing capacity of lung for carbon monoxide percent predicted; SD, standard deviation.

further identify the separation between two groups and to understand the variables responsible for classification. It is generally considered that the variable importance in the projection (VIP) greater than 1 indicates a significant effect on the classification of sample categories. The PLS-DA model between the two groups was established after log₂ log conversion of the data, and the method used for scaling is Par. The seven-fold cross validation was performed during modeling. To evaluate the model, the PLS-DA model was subjected to 200 response permutation tests (RPT) with standard parameters (R₂Y and Q₂). Spearman correlation coefficient can detect more complex correlations, providing clues and evidence for further research and linearization. The commercial database Kyoto Encyclopedia of Genes and Genomes (KEGG) was used for pathway analysis.

Results

Study subjects

Our study included ten male COPD patients and ten controls. There were no significant differences in age or body mass index (BMI) between the two groups of subjects (Table 1). The FVC (%pred), FEV₁ (%pred), FEV₁/FVC ratio and diffusing capacity of lung for carbon monoxide percent predicted [DLCO (%pred)] in non-smokers were greater than those in COPD patients (Table 1), while the TLC (%pred) in non-smokers was less than COPD patients (Table 1).

Mouse COPD model

Increased lung volume parameters (IC, FRC and TLC) and compliance (C_{chord}), and reduced airflow to volume ratio (FEV₂₅/FVC, FEV₅₀/FVC) were observed in CS-exposed mice compared to control mice (Figure 1A-1F). CS-exposed mice demonstrated disruption of alveolar septa and enlarged alveolar spaces compared to control mice (Figure 1G-1H), as indicated by a greater Lm in CS-exposed mice than control mice (Figure 1I).

Metabolites identification

There were 147 metabolites identified between two groups in human lung tissue, including 39 amino acids, 36 fatty acids, seventeen carnitines, sixteen organic acids, fourteen carbohydrates and 25 other metabolites. A total of 211 metabolites were observed in mouse lung tissue including 59 amino acids, 43 fatty acids, 29 organic acids, nineteen carnitines, seventeen carbohydrates and 44 other metabolites. The characteristic metabolite profiles of human and mouse lung tissue samples with good peak-to-peak separation, which indicated that LC-MS/MS was suitable for the determination in this study.

Multivariate analysis of metabolites

According to the quantitative value of each metabolite

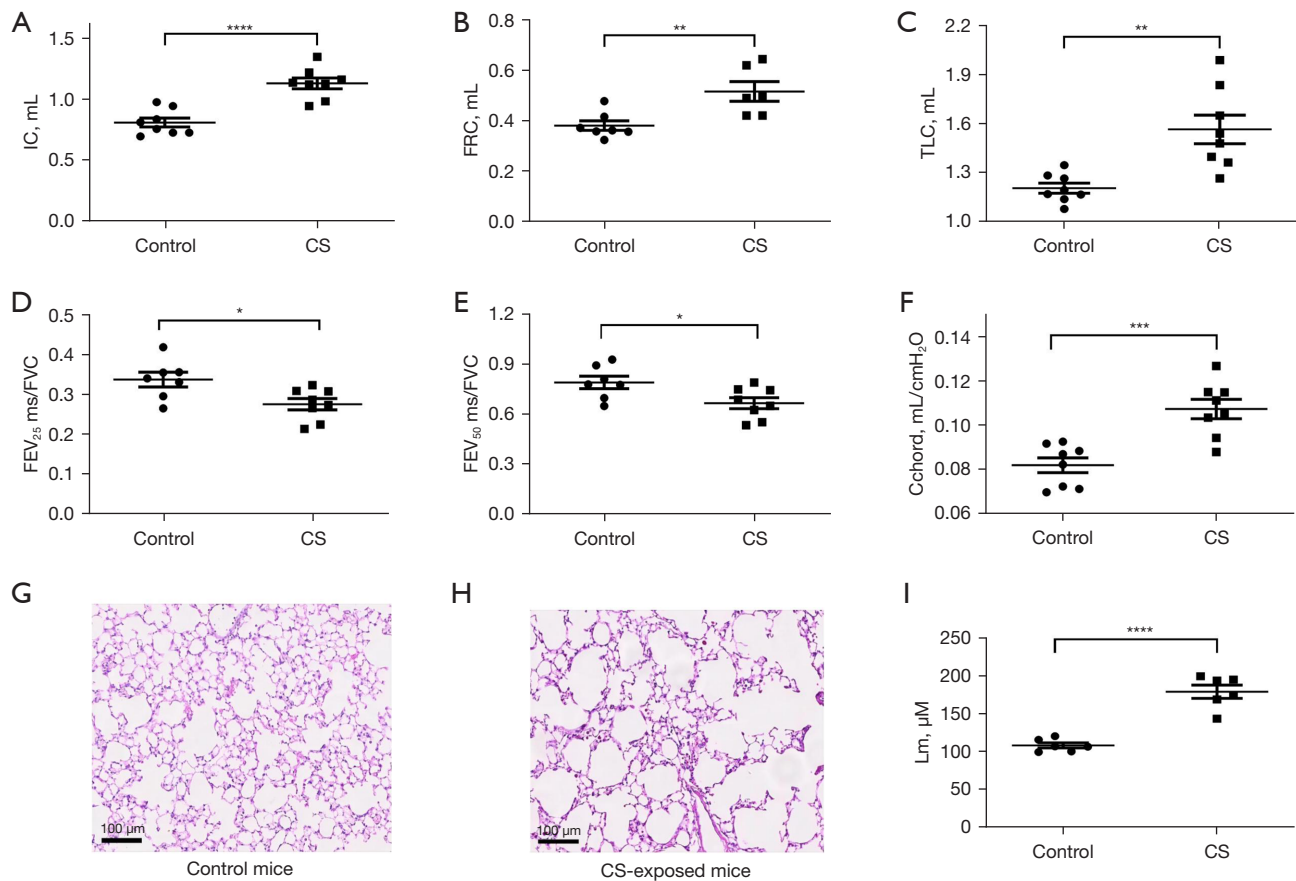


Figure 1 Lung function parameters and HE staining of mice. (A) Individual and mean values of IC. (B) FRC. (C) TLC. (D,E) Percentage of FEV in first 25 and 50 ms of fast expiration (FEV₂₅ and FEV₅₀) of FVC. (F) Cchord. (G,H) HE staining of lung tissue of control mice and CS-exposed mice. (I) Individual and mean values of Lm in lung sections from the two experimental groups. *, $P < 0.05$; **, $P < 0.01$; ***, $P < 0.001$; ****, $P < 0.0001$. HE, haematoxylin-eosin; IC, inspiratory capacity; FRC, functional residual capacity; TLC, total lung capacity; FEV, forced expiratory volume; FVC, forced vital capacity; Cchord, chord compliance; Lm, mean linear intercept; CS, cigarette smoke.

in each sample, the correlation between samples was calculated, and the biological replicates among samples in the group could be observed through the correlation analysis. As seen in *Figure 2A,2B*, the biological replicates were concordant in both human and mouse samples. Clustering of samples within groups was evident and the metabolic differences between groups were significant. There was a distinct separation between COPD and control lungs in both humans and mice (*Figure 2C,2D*), suggesting significant differences in the content or composition of metabolites between these groups. For human lung tissue, the first principal component can explain 19.89% of the features of the original data and the second principal component can explain 18.11% of the features. For mouse lung tissue, the first principal component can explain

27.29% of the features of mouse samples and the second principal component can explain 14.80% of the features. As shown in *Figure 2E,2F*, a further distinct separation between two groups in humans and mice by PLS-DA plot, indicates that the metabolites were significantly changed between groups. The R²Y value of PLS-DA model was 0.94, and the Q² value was -0.04. The intercept of the Y-axis was less than zero by RPT, indicating that the models were not overfitting, and had good prediction ability (*Figure 2G,2H*).

Screening of differential metabolites

Combining ratio analysis and *t*-test analytical methods, a volcano plot was used to show the difference in quantitative values of metabolites between the two groups. Usually,

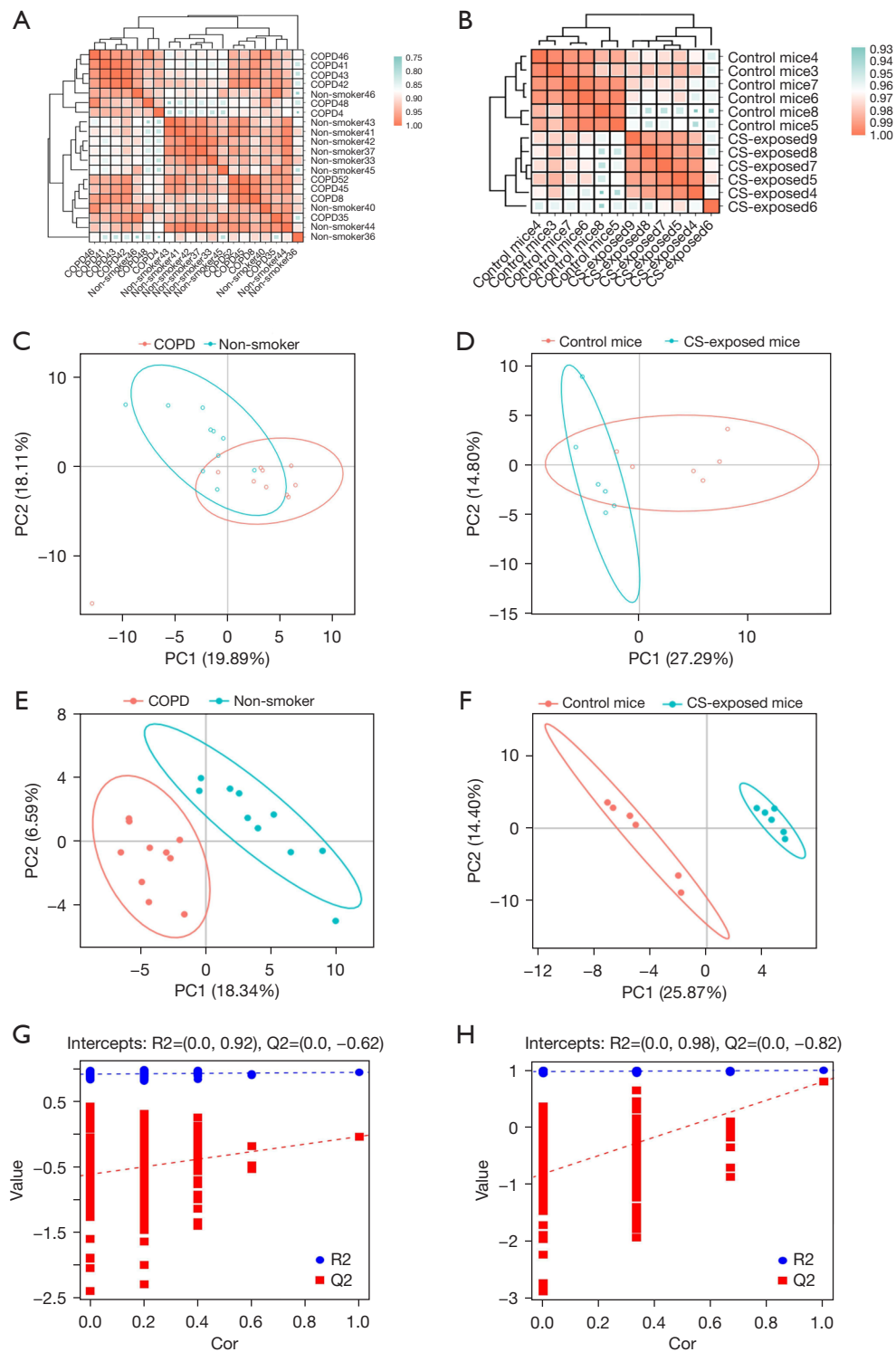


Figure 2 Statistical analysis of metabolic profiles in lung tissues. (A) Sample correlation of human lung tissues. (B) Sample correlation of mouse lung tissues. (C) PCA of human lung tissues. (D) PCA analysis of mouse lung tissues. (E) PLS-DA analysis of human lung tissues. (F) PLS-DA analysis of mouse lung tissues. (G) Response permutation testing of human lung tissue samples. (H) Response permutation testing of mouse lung tissue samples. COPD, chronic obstructive pulmonary disease; CS, cigarette smoke; PC, principal component; Cor, correlation; PCA, principal component analysis; PLS-DA, partial least squares-discriminant analysis.

ratio ≥ 1.2 or ratio ≤ 0.83 and P value < 0.05 were used as the criteria for screening differential metabolites. In addition, to have an intuitive understanding of the differential metabolites in each sample, hierarchical clustering heat maps of differential metabolites were drawn in *Figure 3A, 3B*, indicating the concentrations of multiple metabolites in human and mouse lung tissues were significantly different between these groups (*Figure 3C, 3D*).

Based on the ratio and P value, 22 metabolites were up-regulated and eleven metabolites were down-regulated in COPD patients compared to controls (*Figure 3E, 3F*). The complete list of differential metabolites of human samples is shown in *Table S1*. They were grouped into four broad categories: amino acids, carbohydrates, carnitines and other metabolites, which highlighted that COPD was relevant to the disorder of amino acid, carbohydrate and lipid metabolism. The levels of leucine, glutamic acid, isoleucine and linoleylcarnitine were decreased, while the contents of glycine, aspartic acid, gamma-aminobutyric acid (GABA), 1-methylhistidine, fumaric acid, malic acid and propionylcarnitine were increased. There were 35 metabolites up-regulated and 28 metabolites down-regulated between the two groups in mice (*Figure 3G, 3H*). The complete list of the changed metabolites of mouse samples is displayed in *Table S2*, including amino acids, fatty acids, organic acids and other metabolites. The concentrations of arginine, leucine, isoleucine, serine, threonine and malonylcarnitine were higher in CS-exposed mice, while the levels of lactic acid, adrenic acid, alpha-Linolenic acid, gamma-Linolenic acid, palmitic acid and other polyunsaturated fatty acids were lower in CS-exposed mice. These results indicate that dysregulation of amino acids and fatty acids might be involved in the process of COPD.

Metabolic pathway analysis

A metabolic pathway enrichment analysis of differential metabolites was performed based on KEGG. The metabolic pathway with P value less than 0.05 was considered as significantly enriched, with the smaller the P value, the higher the degree of enrichment. Bubble plots were drawn for the pathway with significantly enriched differential metabolites in human and mouse samples (*Figure 4*).

There were 63 metabolic pathways in total between COPD patients and healthy controls that were differentially expressed, mainly involving those in substance metabolism, energy production and an imbalance of oxidation and antioxidation. There were 12 pathways associated with

amino acid metabolism disorder, including glycine, serine and threonine metabolism, and valine, leucine and isoleucine biosynthesis and degradation pathway. There were six pathways regarding energy metabolism dysfunction such as oxidative phosphorylation, pentose phosphate pathway and tricarboxylic acid (TCA) cycle. Changes in cellular redox status were reflected in those of glutathione (GSH) metabolism, forkhead transcription factor O (FOXO) signaling pathway, and nitrogen metabolism pathways. Overall, these results indicate the presence of abnormalities of amino acid metabolism, energy production and oxidative stress may play key roles in the pathogenesis of COPD.

There were 41 differential metabolic pathways in total between the two groups of mice with thirteen pathways related to amino acid metabolism such as biosynthesis of amino acids, and arginine and proline metabolism. Compared with human COPD, more evident lipid metabolism changes occurred in CS-exposed mice. There were four lipid metabolism pathways including biosynthesis of unsaturated fatty acids, linoleic acid metabolism, fatty acid biosynthesis and fatty acid degradation. There were also disordered energy related pathways like glycolysis and hypoxia-inducible factor-1 (HIF-1) signaling pathway. These results indicate that amino acid, fatty acid, and energy metabolism might be potential pathways for COPD development in the mouse model.

Overlapping changes in lung tissues of humans and mice

Based on the metabolomics and KEGG pathway analysis results, carnitine metabolism and the ferroptosis pathway changed both in human and mice lung tissues. Metabolomics revealed that propionylcarnitine was upregulated and linoleylcarnitine was downregulated in COPD patients, while malonylcarnitine and adipoylcarnitine were upregulated in CS-exposed mice (*Figure 5*).

Correlations between metabolites and lung function parameters

We performed correlation analysis on the expression of metabolites with lung function parameters. Negative correlations were observed between FEV₁% predicted and propionylcarnitine levels and between FEV₁/FVC% and glycine levels in the human samples. A positive correlation was found between FEV₁/FVC% and leucine and glutamic acid levels (*Table 2*). There were positive correlations between

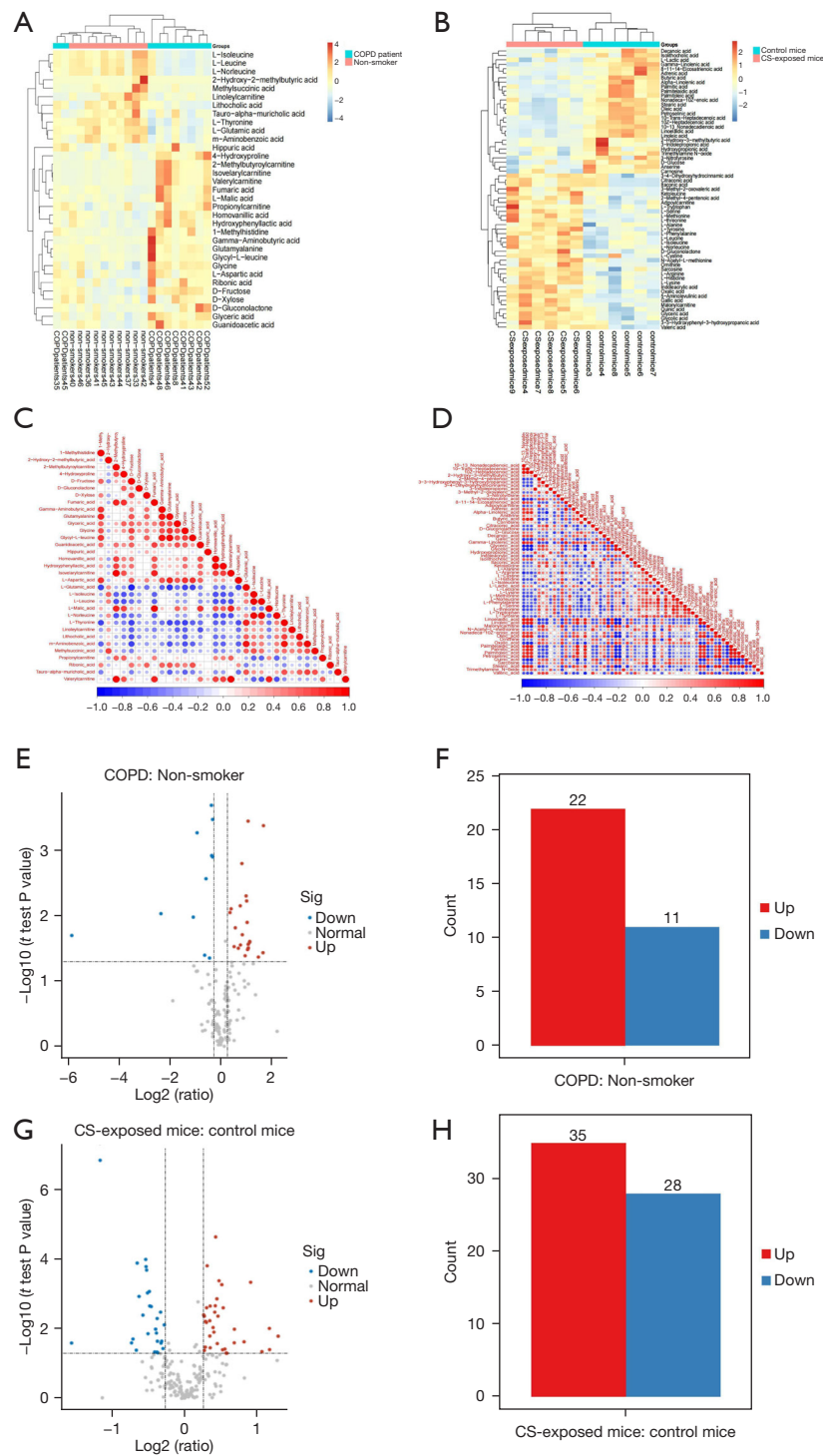


Figure 3 Differential metabolite analysis in lung tissues. (A) Human differential metabolite clustering heatmap. (B) Mouse differential metabolite clustering heatmap (red indicated higher expression level and blue lower expression level). (C) Correlation analysis for human differential metabolites. (D) Correlation analysis for mouse differential metabolites (both the x-axis and y-axis represent the metabolites name, and the scale bar from “-1.0 to 1.0” represents the correlation coefficient. Red represented a positive correlation between the two metabolites, blue represented a negative correlation between the two metabolites). (E) Human metabolites volcano plot. (F) Human differential metabolite statistical bar chart. (G) Mouse metabolites volcano plot. (H) Mouse differential metabolite statistical bar chart. COPD, chronic obstructive pulmonary disease; CS, cigarette smoke.

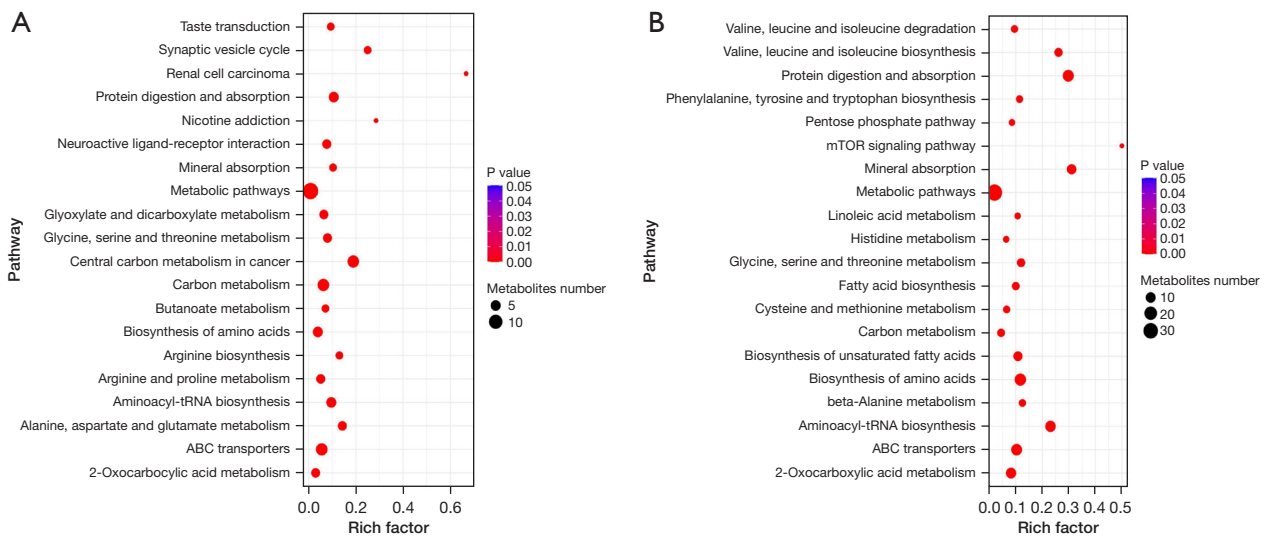


Figure 4 Metabolic pathway analysis. (A) Human metabolic pathway enrichment bubble plots. (B) Mouse metabolic pathway enrichment analysis bubble plots. The vertical axis is the name of metabolic pathway, and the horizontal axis is enrichment factor, which refers to the proportion of differential metabolites in total metabolites in this pathway. The greater the rich factor, the greater the enrichment degree. The bubble color from blue to red indicates that P value increases successively. The larger the bubble, the more metabolites enriched on the pathway.

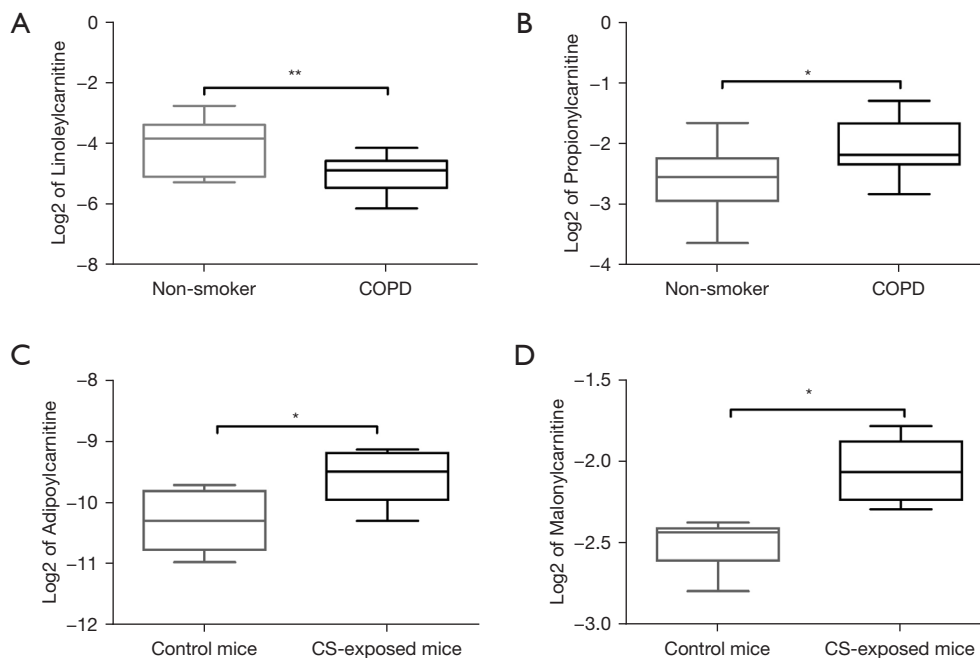


Figure 5 Acyl-carnitine contents were significantly different in lung tissues between two groups. (A) Log₂ of Linoleylcarnitine in human lung tissues; (B) Log₂ of Propionylcarnitine in human lung tissues; (C) Log₂ of Adipoylcarnitine in mouse tissues; (D) Log₂ of Malonylcarnitine in mouse tissues. *, P<0.05; **, P<0.01. COPD, chronic obstructive pulmonary disease; CS, cigarette smoke.

Table 2 Correlation between lung metabolites and lung function parameters in human participants

Lung function parameters	Values	Leucine	Glutamic acid	Linoleylcarnitine	Glycine	Propionylcarnitine	Fumaric acid	Malic acid
FVC (%pred)	r	0.496*	0.377	0.227	-0.073	-0.283	-0.356	0.005
	P	0.026	0.101	0.336	0.758	0.227	0.123	0.985
FEV ₁ (%pred)	r	0.714**	0.650*	0.373	-0.046	-0.445*	-0.589**	-0.371
	P	<0.01	0.02	0.105	0.076	0.049	0.006	0.107
FEV ₁ /FVC (%)	r	0.501*	0.568**	0.331	-0.453*	-0.432	-0.420	-0.477*
	P	0.025	0.009	0.154	0.045	0.057	0.066	0.034
TLC (%pred)	r	-0.619**	-0.373	-0.131	0.302	0.358	0.371	0.451*
	P	0.004	0.106	0.582	0.196	0.121	0.107	0.046
DLCO (%pred)	r	0.648**	0.542*	0.338	-0.438	-0.433	-0.466*	-0.528*
	P	0.002	0.014	0.145	0.054	0.056	0.038	0.017

*, P<0.05; **, P<0.01. FVC (%pred), forced vital capacity percent predicted; FEV₁ (%pred), forced expiratory volume in one second percent predicted; TLC (%pred), total lung capacity percent predicted; DLCO (%pred), diffusing capacity of lung for carbon monoxide percent predicted.

Table 3 Correlation between metabolites and lung function parameters in mice

Lung function parameters	Values	Arginine	Leucine	Phenylalanine	α -Linolenic acid	Palmitic acid	Linoleic acid	Adipoylcarnitine	Malonylcarnitine
FEV ₂₅ /FVC	r	-0.582*	-0.284	-0.476	0.775**	0.648*	0.767**	-0.378	-0.566
	P	0.047	0.371	0.118	0.003	0.023	0.004	0.225	0.055
FEV ₅₀ /FVC	r	-0.576	-0.274	-0.431	0.693*	0.582*	0.734**	-0.404	-0.561
	P	0.050	0.389	0.161	0.012	0.047	0.007	0.193	0.058
FRC	r	0.375	0.213	0.646*	-0.375	-0.227	-0.172	-0.168	0.399
	P	0.230	0.506	0.023	0.230	0.478	0.592	0.601	0.198
IC	r	0.838**	0.575	0.714**	-0.788**	-0.630*	-0.832**	0.545	0.765*
	P	0.001	0.051	0.009	0.002	0.028	0.001	0.067	0.004
TLC	r	0.796**	0.529	0.807**	-0.758**	-0.577*	-0.712**	0.356	0.749**
	P	0.002	0.077	0.002	0.004	0.049	0.009	0.256	0.005
Cchord	r	0.799**	0.489	0.590*	-0.780**	-0.681*	-0.826**	0.555	0.722**
	P	0.002	0.106	0.043	0.003	0.015	0.001	0.061	0.008

*, P<0.05; **, P<0.01. FEV₂₅/FVC and FEV₅₀/FVC, percentage of forced expiratory volume in first 25 and 50 ms of fast expiration of forced vital capacity; FRC, functional residual capacity; IC, individual and mean values of inspiratory capacity; TLC, total lung capacity; Cchord, chord compliance.

malonylcarnitine and IC, TLC, and Cchord in the mice (*Table 3*).

Discussion

A nationwide prevalence study revealed that the prevalence

of COPD in men is more than twice that of women (19), therefore, we examined and compared the levels of metabolites in lung tissues from male COPD patients and CS induced male mice model of COPD to their respective controls measured by targeted HM350 metabolomics. We

found that several classes of metabolites were abnormally expressed. Pathway analysis by KEGG identified disturbed pathways with 22 and 35 metabolites up-regulated and eleven and 28 metabolites down-regulated respectively in COPD patients and in mice COPD model. Metabolites such as amino acids, carbohydrates and carnitines changed in both COPD patients and mice, indicating disorders of amino acid pathways and energy production pathways although the specific amino acids and carbohydrates were different in the patients and mice. These altered metabolites observed in COPD are an indication of the processes of aging, apoptosis, oxidative stress and inflammation that occurs in COPD.

In this study, amino acids were different between the two groups in human samples, so were amino acids metabolic pathways such as glycine, serine and threonine metabolism pathway and biosynthesis of amino acids pathway. Several studies have reported significant decrease in serum levels of branched-chain amino acids (BCAA) in individuals with COPD (20,21). Leucine and isoleucine are both BCAA, and their biosynthetic processes promote protein anabolism and maintain glucose homeostasis in skeletal muscle (22). Consistently, the levels of leucine and isoleucine were notably decreased in COPD patients in the present study. Low leucine levels lead to loss of appetite, protein and mineral malabsorption, poor growth and weight loss, which might affect skeletal muscle function and result in poor pulmonary ventilation. There were positive correlations between the leucine levels and FVC%, FEV₁%, FEV₁/FVC%, and DLCO%, and a negative correlation between the leucine levels and TLC. In addition, decreased leucine is involved in the mammalian target of rapamycin (mTOR) signaling pathway which is related to aging and autophagy. Therefore, down-regulated leucine may influence the development of COPD through cell apoptosis and senescence by mTOR complex 1 (mTORC1) signaling pathway (23).

Contrary to human samples, there were some differences in amino acid metabolism in COPD mice. Both leucine and isoleucine were increased in CS-exposed mice, which was very different from COPD human. A study reported leucine stimulated mTORC1 to regulate cell growth and autophagy via the mTOR pathway (24). Reduced leucine levels were also observed in Sprague-Dawley rats lung tissues after three, eight and 21 days of CS exposure (25). The explanation may be species difference and CS exposure duration.

Glutamic acid was down-regulated in COPD subjects

compared to controls, which could influence the FOXO signaling pathway. Hwang *et al.* reported that uncontrolled regulation of FOXO protein acetylation leads to increased inflammatory response, cell senescence and apoptosis (23). In addition, glutamic acid is involved in the ferroptosis in COPD patients, which is a novel programmed cell death process characterized by mitochondrial contraction, lipid peroxidation, reactive oxygen species (ROS) and iron ions accumulation, and GSH contents decline (26,27). Glutamic acid can be used to synthesize GSH, and the latter is a major endogenous antioxidant and plays an important role in the regulation of redox status (28). The decrease of GSH synthesis could reduce phospholipid-hydroperoxide glutathione peroxidase (GPX4) activity and elevate oxidative stress (29). On the contrary, cysteine was up-regulated in CS-exposed mice. Cysteine can also be used to synthesize GSH (30). The activity of GPX4 is negatively related to ROS accumulation and lipid peroxidation increase during CS exposure. Yoshida *et al.* showed that the reduction of GPX4 enhanced cell lipid peroxidation and cell death, and GPX4-GSH axis was crucial to the regulation of ferroptosis in COPD by increasing lipid peroxidation, cell death and oxidative stress (31). Additionally, there were positive correlations between glutamic acid levels and FEV₁%, FEV₁/FVC%, and DLCO% in the current study. Thus, decreased glutamic acid might be involved in COPD by dysregulating FOXO signaling molecule and ferroptosis pathway, and reducing lung function.

Phenylalanine, a glycolytic and ketogenic amino acid, was high in lungs of COPD mice, and its metabolic levels can reflect protein synthesis and degradation state (32). A previous research showed heightened levels of phenylalanine in emphysema patients, and phenylalanine was closely associated with elevated inflammatory levels (33). In our study, phenylalanine had positive correlations with FRC, IC, TLC and Cchord in COPD mice.

There is an altered TCA cycle in COPD patients (34). In our study, the intermediates of TCA such as fumaric acid and malic acid were increased, which indicated TCA disturbances. The accumulated intermediates are unable to enter the next circulation consumption, causing a reduction in adenosine triphosphate (ATP) synthesis. In the present study, fumaric acid was negative with FEV₁% and DLCO%, and malic acid was negative with FEV₁/FVC% and DLCO% while positive with TLC%. Thus, the altered TCA causing energy deficiency might be one of the reasons for COPD development.

Increased oxidative stress after long-term exposure to CS

could damage energy metabolism homeostasis and render lung malfunction (35,36). The oxidative stress burden is aggravated in COPD due to the overproduction of ROS and reactive nitrogen species (RNS) (37). Arginine metabolism is a known primary source of RNS (38). In our study, arginine was up-regulated in COPD mice, and arginine was negatively correlated with FEV₂₅/FVC and FEV₅₀/FVC and positively correlated with IC, TLC and Cchord. Thus the change of arginine metabolism might impair airway physiological functions, leading to the development of COPD. Xu *et al.* also observed elevated arginine levels accompanied by increased oxidative stress and inflammatory signaling in asthmatic patients (39). These results indicate that arginine could affect airway function, oxidative stress and inflammation, further influencing the development of COPD.

Fatty acids are one of the most important lipids in the body, and fatty acid oxidation (FAO) mainly occurs in mitochondria and eventually produces acetyl-CoA after shuttle process and a series of enzymatic reactions (40). Carnitine, a compound involved in acyl-transfer, plays an important role in regulating mitochondrial β -oxidation as it imports fatty acids into mitochondria for subsequent FAO (41). Therefore, the disturbance of carnitine has been considered the basis of FAO change (42). Conlon *et al.* showed that the content of L-carnitine was reduced in murine model of elastase-induced emphysema and L-carnitine supplement could protect cells from apoptosis (41). Salama *et al.* found that L-carnitine could improve potassium dichromate induced acute lung injury by regulating cellular oxidative stress and inflammatory response (43). Long and very long chain acylcarnitine increased with age, indicating that decreased mitochondrial activity could lead to increased plasma acylcarnitine (44). In the present study, significant changes in acylcarnitines metabolism were observed in both lung tissues derived from COPD patients and mice. Propionylcarnitine was up-regulated and linoleylcarnitine was down-regulated in COPD patients. Additionally, the propionylcarnitine levels were negatively associated with FEV₁%. We also discovered the abnormality of the carnitine shuttle in the lungs of COPD mice. Malonylcarnitine levels were increased, and were positively correlated with IC, TLC and Cchord. Thus, abnormal acylcarnitines metabolism due to impaired mitochondria may break the balance of β -oxidation, lead to mitochondrial damage, oxidative stress, apoptosis and enhance the development of COPD (12). Inhibiting acylcarnitine contents to reduce oxidative stress and aging might potentially attenuate COPD.

In our study, PUFA were decreased in COPD mice, but not in the human COPD tissues, which may be explained by species differences or technique sensitivity and limitation. Such as linoleic acid, α -Linolenic acid, oleic acid, palmitic acid and stearic acid were reduced in COPD mice. PUFA could convert into a variety of different pro-inflammatory mediators, such as leukotriene and prostaglandins under the catalysis of a series of enzymes [cyclooxygenase (COX), lipoxygenase (LOX) and cytochrome P450 (CYP450) etc.], which promote inflammation and transmit signaling by receptor-mediated mechanisms (45). PUFA are also particularly sensitive to oxidative injury, the reduced lipids reflected an increased level of oxidative stress after CS exposure (46). Linoleic acid, α -Linolenic acid and palmitic acid had positive correlations with FEV₂₅/FVC and FEV₅₀/FVC, and negative correlations with IC, TLC and Cchord. These data indicate that PUFA down-regulation was associated with high levels of inflammation, oxidative stress, and lung function dysregulation in COPD mice.

Although COPD patients and COPD mice shared some similarities in lung pathology and lung function, including increased infiltration of lung parenchymal cells, airway epithelial thickening, airway remodeling (matrix deposition and fibrosis), emphysema (alveolar space expanding) and reduced lung function (47). However, there are some differences due to the species. Compared to human, mice had few submucosal glands, less extensive branching, less goblet cells and respiratory bronchioles (48). The bronchoalveolar lavage fluid (BALF) from CS-exposed mice was positively correlated with human COPD BALF with 2,040 metabolites in common, suggesting that mouse models can be used to interrogate human lung metabolome changes. CS-exposed mice had increased glycerolipids and glycerophospholipids in plasma and BALF (49). In this study, we compared the metabolites between COPD patients and mice and found that metabolites such as BCAA and carnitine were changed in both COPD patients and mice, and the pathways regarding aging, apoptosis and oxidative stress such as mTOR and ferroptosis were also altered in both COPD patients and mice. While compared with human, different kinds of amino acids, and more remarkable changes of lipid metabolism and related inflammatory response in CS-exposed mice, indicating that the use of COPD mouse model to study diseases has some limitations. The differences in metabolites between COPD mice and humans suggest that COPD mouse model cannot fully mimic human disease progression. Therefore, the conclusions should be cautious when we used the COPD

mouse model to discover biomarkers for COPD diagnosis and to investigate potential pathogenesis.

There are strengths and limitations in this study. Many studies have determined the metabolic characteristics of COPD in blood and BALF, but few studies have reported metabolic changes in lung tissue. We used lung tissue for study, as it can better present the metabolic characteristics of COPD. In addition, we also compared the differential metabolites between COPD patients and COPD mice. The limitations in this study include small sample size, male patients only, mild-moderate disease severity, and lack of a smoker group, which may ignore the effect of smoking on metabolites. Therefore, more in-depth experimental studies are needed for further verification.

Conclusions

There were differences in metabolites between COPD and control by HM350 metabolomics. Amino acids, carbohydrates and carnitines were changed in both COPD patients and mice, while PUFA metabolism was changed only in COPD mice. Furthermore, we also investigated acylcarnitines metabolism and ferroptosis pathway as overlapping metabolic changes in COPD patients and mice. These altered metabolites involved in COPD through aging, apoptosis, oxidative stress and inflammation, indicating that the above dysregulation may be related to the development of COPD. Based on these disordered metabolites and pathways, our study may reveal the potential pathogenesis of COPD.

Acknowledgments

Funding: This work was supported by the projects of the National Nature Science Foundation of China (Nos. 81870031 and 82070041), and Shanghai Municipal Health Commission (No. 2020YJZX0115).

Footnote

Reporting Checklist: The authors have completed the ARRIVE reporting checklist. Available at <https://jtd.amegroups.com/article/view/10.21037/jtd-22-1731/rc>

Data Sharing Statement: Available at <https://jtd.amegroups.com/article/view/10.21037/jtd-22-1731/dss>

Peer Review File: Available at <https://jtd.amegroups.com/>

[article/view/10.21037/jtd-22-1731/prf](https://jtd.amegroups.com/article/view/10.21037/jtd-22-1731/prf)

Conflicts of Interest: All authors have completed the ICMJE uniform disclosure form (available at <https://jtd.amegroups.com/article/view/10.21037/jtd-22-1731/coif>). The authors have no conflicts of interest to declare.

Ethical Statement: The authors are accountable for all aspects of the work in ensuring that questions related to the accuracy or integrity of any part of the work are appropriately investigated and resolved. The study was conducted in accordance with the Declaration of Helsinki (as revised in 2013). This study was approved by the Institutional Ethics Committee of Shanghai Chest Hospital (No. KS1969), and written informed consent was obtained from all subjects. Experiments were performed under a project license (No. KS1969) granted by the Institutional Ethics Committee of Shanghai Chest Hospital, in compliance with the institutional laboratory animal management guidelines for the care and use of animals.

Open Access Statement: This is an Open Access article distributed in accordance with the Creative Commons Attribution-NonCommercial-NoDerivs 4.0 International License (CC BY-NC-ND 4.0), which permits the non-commercial replication and distribution of the article with the strict proviso that no changes or edits are made and the original work is properly cited (including links to both the formal publication through the relevant DOI and the license). See: <https://creativecommons.org/licenses/by-nc-nd/4.0/>.

References

1. GBD Chronic Respiratory Disease Collaborators. Prevalence and attributable health burden of chronic respiratory diseases, 1990–2017: a systematic analysis for the Global Burden of Disease Study 2017. *Lancet Respir Med* 2020;8:585–96.
2. Viegi G, Maio S, Fasola S, Baldacci S. Global Burden of Chronic Respiratory Diseases. *J Aerosol Med Pulm Drug Deliv* 2020;33:171–7.
3. Vestbo J, Mathioudakis AG. The emerging Chinese COPD epidemic. *Lancet* 2018;391:1642–3.
4. Ten VS, Ratner V. Mitochondrial bioenergetics and pulmonary dysfunction: Current progress and future directions. *Paediatr Respir Rev* 2020;34:37–45.
5. Michaeloudes C, Bhavsar PK, Mumby S, et al. Role of Metabolic Reprogramming in Pulmonary Innate

- Immunity and Its Impact on Lung Diseases. *J Innate Immun* 2020;12:31-46.
6. Wang C, Li JX, Tang D, et al. Metabolic changes of different high-resolution computed tomography phenotypes of COPD after budesonide-formoterol treatment. *Int J Chron Obstruct Pulmon Dis* 2017;12:3511-21.
 7. Ren X, Zhang J, Fu X, et al. LC-MS based metabolomics identification of novel biomarkers of tobacco smoke-induced chronic bronchitis. *Biomed Chromatogr* 2016;30:68-74.
 8. Kilk K, Aug A, Ottas A, et al. Phenotyping of Chronic Obstructive Pulmonary Disease Based on the Integration of Metabolomes and Clinical Characteristics. *Int J Mol Sci* 2018;19:666.
 9. Ren X, Ma S, Wang J, et al. Comparative effects of dexamethasone and bergenin on chronic bronchitis and their anti-inflammatory mechanisms based on NMR metabolomics. *Mol Biosyst* 2016;12:1938-47.
 10. van der Does AM, Heijink M, Mayboroda OA, et al. Dynamic differences in dietary polyunsaturated fatty acid metabolism in sputum of COPD patients and controls. *Biochim Biophys Acta Mol Cell Biol Lipids* 2019;1864:224-33.
 11. Zhao P, Li J, Li Y, et al. Integrating Transcriptomics, Proteomics, and Metabolomics Profiling with System Pharmacology for the Delineation of Long-Term Therapeutic Mechanisms of Bufei Jianpi Formula in Treating COPD. *Biomed Res Int* 2017;2017:7091087.
 12. Jiang Z, Knudsen NH, Wang G, et al. Genetic Control of Fatty Acid β -Oxidation in Chronic Obstructive Pulmonary Disease. *Am J Respir Cell Mol Biol* 2017;56:738-48.
 13. Kim HY, Lee HS, Kim IH, et al. Comprehensive Targeted Metabolomic Study in the Lung, Plasma, and Urine of PPE/LPS-Induced COPD Mice Model. *Int J Mol Sci* 2022;23:2748.
 14. Vlahos R, Bozinovski S. Preclinical murine models of Chronic Obstructive Pulmonary Disease. *Eur J Pharmacol* 2015;759:265-71.
 15. Zhang H, Li C, Song X, et al. Integrated analysis reveals lung fibrinogen gamma chain as a biomarker for chronic obstructive pulmonary disease. *Ann Transl Med* 2021;9:1765.
 16. Sasaki M, Chubachi S, Kameyama N, et al. Evaluation of cigarette smoke-induced emphysema in mice using quantitative micro-computed tomography. *Am J Physiol Lung Cell Mol Physiol* 2015;308:L1039-45.
 17. Li Y, Yu G, Yuan S, et al. Cigarette Smoke-Induced Pulmonary Inflammation and Autophagy Are Attenuated in Ephx2-Deficient Mice. *Inflammation* 2017;40:497-510.
 18. Li F, Xu M, Wang M, et al. Roles of mitochondrial ROS and NLRP3 inflammasome in multiple ozone-induced lung inflammation and emphysema. *Respir Res* 2018;19:230.
 19. Fang L, Gao P, Bao H, et al. Chronic obstructive pulmonary disease in China: a nationwide prevalence study. *Lancet Respir Med* 2018;6:421-30.
 20. Kuo WK, Liu YC, Chu CM, et al. Amino Acid-Based Metabolic Indexes Identify Patients With Chronic Obstructive Pulmonary Disease And Further Discriminates Patients In Advanced BODE Stages. *Int J Chron Obstruct Pulmon Dis* 2019;14:2257-66.
 21. Labaki WW, Gu T, Murray S, et al. Serum amino acid concentrations and clinical outcomes in smokers: SPIROMICS metabolomics study. *Sci Rep* 2019;9:11367.
 22. Zhou J, Li Q, Liu C, et al. Plasma Metabolomics and Lipidomics Reveal Perturbed Metabolites in Different Disease Stages of Chronic Obstructive Pulmonary Disease. *Int J Chron Obstruct Pulmon Dis* 2020;15:553-65.
 23. Hwang JW, Yao H, Caito S, et al. Redox regulation of SIRT1 in inflammation and cellular senescence. *Free Radic Biol Med* 2013;61:95-110.
 24. Jewell JL, Kim YC, Russell RC, et al. Metabolism. Differential regulation of mTORC1 by leucine and glutamine. *Science* 2015;347:194-8.
 25. Barupal DK, Pinkerton KE, Hood C, et al. Environmental Tobacco Smoke Alters Metabolic Systems in Adult Rats. *Chem Res Toxicol* 2016;29:1818-27.
 26. Dixon SJ, Lemberg KM, Lamprecht MR, et al. Ferroptosis: an iron-dependent form of nonapoptotic cell death. *Cell* 2012;149:1060-72.
 27. Battaglia AM, Chirillo R, Aversa I, et al. Ferroptosis and Cancer: Mitochondria Meet the "Iron Maiden" Cell Death. *Cells* 2020;9:1505.
 28. Otasevic V, Vucetic M, Grigorov I, et al. Ferroptosis in Different Pathological Contexts Seen through the Eyes of Mitochondria. *Oxid Med Cell Longev* 2021;2021:5537330.
 29. Fläring UB, Rooyackers OE, Wernerman J, et al. Glutamine attenuates post-traumatic glutathione depletion in human muscle. *Clin Sci (Lond)* 2003;104:275-82.
 30. Zhao H, Dennery PA, Yao H. Metabolic reprogramming in the pathogenesis of chronic lung diseases, including BPD, COPD, and pulmonary fibrosis. *Am J Physiol Lung Cell Mol Physiol* 2018;314:L544-54.
 31. Yoshida M, Minagawa S, Araya J, et al. Involvement of cigarette smoke-induced epithelial cell ferroptosis in

- COPD pathogenesis. *Nat Commun* 2019;10:3145.
32. Jonker R, Deutz NE, Erbland ML, et al. Effectiveness of essential amino acid supplementation in stimulating whole body net protein anabolism is comparable between COPD patients and healthy older adults. *Metabolism* 2017;69:120-9.
 33. Ubhi BK, Riley JH, Shaw PA, et al. Metabolic profiling detects biomarkers of protein degradation in COPD patients. *Eur Respir J* 2012;40:345-55.
 34. Xue M, Zeng Y, Lin R, et al. Metabolomic profiling of anaerobic and aerobic energy metabolic pathways in chronic obstructive pulmonary disease. *Exp Biol Med (Maywood)* 2021;246:1586-96.
 35. Kirkham PA, Barnes PJ. Oxidative stress in COPD. *Chest* 2013;144:266-73.
 36. Rahman I. The role of oxidative stress in the pathogenesis of COPD: implications for therapy. *Treat Respir Med* 2005;4:175-200.
 37. Bernardo I, Bozinovski S, Vlahos R. Targeting oxidant-dependent mechanisms for the treatment of COPD and its comorbidities. *Pharmacol Ther* 2015;155:60-79.
 38. Aydin M, Altintas N, Cem Mutlu L, et al. Asymmetric dimethylarginine contributes to airway nitric oxide deficiency in patients with COPD. *Clin Respir J* 2017;11:318-27.
 39. Xu W, Ghosh S, Comhair SA, et al. Increased mitochondrial arginine metabolism supports bioenergetics in asthma. *J Clin Invest* 2016;126:2465-81.
 40. Wang M, Wang K, Liao X, et al. Carnitine Palmitoyltransferase System: A New Target for Anti-Inflammatory and Anticancer Therapy? *Front Pharmacol* 2021;12:760581.
 41. Conlon TM, Bartel J, Ballweg K, et al. Metabolomics screening identifies reduced L-carnitine to be associated with progressive emphysema. *Clin Sci (Lond)* 2016;130:273-87.
 42. Sharma S, Sud N, Wiseman DA, et al. Altered carnitine homeostasis is associated with decreased mitochondrial function and altered nitric oxide signaling in lambs with pulmonary hypertension. *Am J Physiol Lung Cell Mol Physiol* 2008;294:L46-56.
 43. Salama A, Fayed HM, Elgohary R. L-carnitine alleviated acute lung injuries induced by potassium dichromate in rats: involvement of Nrf2/HO-1 signaling pathway. *Heliyon* 2021;7:e07207.
 44. Jarrell ZR, Smith MR, Hu X, et al. Plasma acylcarnitine levels increase with healthy aging. *Aging (Albany NY)* 2020;12:13555-70.
 45. Calder PC. Dietary modification of inflammation with lipids. *Proc Nutr Soc* 2002;61:345-58.
 46. De Castro J, Hernández-Hernández A, Rodríguez MC, et al. Comparison of changes in erythrocyte and platelet phospholipid and fatty acid composition and protein oxidation in chronic obstructive pulmonary disease and asthma. *Platelets* 2007;18:43-51.
 47. Ghorani V, Boskabady MH, Khazdair MR, et al. Experimental animal models for COPD: a methodological review. *Tob Induc Dis* 2017;15:25.
 48. Fricker M, Deane A, Hansbro PM. Animal models of chronic obstructive pulmonary disease. *Expert Opin Drug Discov* 2014;9:629-45.
 49. Cruickshank-Quinn C, Powell R, Jacobson S, et al. Metabolomic similarities between bronchoalveolar lavage fluid and plasma in humans and mice. *Sci Rep* 2017;7:5108.

Cite this article as: Feng Y, Xie M, Liu Q, Weng J, Wei L, Chung KF, Adcock IM, Chang Q, Li M, Huang Y, Zhang H, Li F. Changes in targeted metabolomics in lung tissue of chronic obstructive pulmonary disease. *J Thorac Dis* 2023;15(5):2544-2558. doi: 10.21037/jtd-22-1731

Table S1 Differential metabolites in human lung tissues

Metabolites	Regulation
1-Methylhistidine	Up
Gamma-Aminobutyric acid	Up
Glycyl-L-leucine	Up
2-Methylbutyrylcarnitine	Up
D-Gluconolactone	Up
Valerylcarnitine	Up
Isovalerylcarnitine	Up
D-Fructose	Up
Guanidoacetic acid	Up
Hydroxyphenyllactic acid	Up
Glutamyalanine	Up
4-Hydroxyproline	Up
Hippuric acid	Up
Homovanillic acid	Up
Glyceric acid	Up
Ribonic acid	Up
L-Malic acid	Up
D-Xylose	Up
Fumaric acid	Up
Propionylcarnitine	Up
L-Aspartic acid	Up
Glycine	Up
L-Leucine	Down
L-Isoleucine	Down
L-Glutamic acid	Down
L-Norleucine	Down
Lithocholic acid	Down
m-Aminobenzoic acid	Down
Tauro-alpha-muricholic acid	Down
L-Thyronine	Down
Linoleylcarnitine	Down
Methylsuccinic acid	Down
2-Hydroxy-2-methylbutyric acid	Down

Table S2 Differential metabolites in mouse lung tissues

Metabolites	Regulation
Ketoleucine	Up
Citraconic acid	Up
3-Methyl-2-oxovaleric acid	Up
Itaconic acid	Up
Gallic acid	Up
Ornithine	Up
L-Histidine	Up
Adipoylcarnitine	Up
L-Tryptophan	Up
Valeric acid	Up
L-Cystine	Up
L-Methionine	Up
N-Acetyl-L-methionine	Up
L-Arginine	Up
L-Tyrosine	Up
2-Methyl-4-pentenoic acid	Up
Sarcosine	Up
Malonylcarnitine	Up
5-Aminolevulinic acid	Up
L-Phenylalanine	Up
Oxalic acid	Up
D-Gluconolactone	Up
L-Lysine	Up
3-4-Dihydroxyhydrocinnamic acid	Up
L-Norleucine	Up
Indoleacrylic acid	Up
Glycolic acid	Up
L-Serine	Up
Glyceric acid	Up
Quinic acid	Up
L-Isoleucine	Up
3-3-Hydroxyphenyl-3-hydroxypropanoic acid	Up
L-Alanine	Up
L-Leucine	Up
L-threonine	Up

Table S2 (*continued*)**Table S2** (*continued*)

Metabolites	Regulation
D-Glucose	Down
Carnosine	Down
Decanoic acid	Down
L-Lactic acid	Down
Palmitelaidic acid	Down
Isolithocholic acid	Down
Palmitic acid	Down
Palmitoleic acid	Down
3-Nitrotyrosine	Down
Butyric acid	Down
Adrenic acid	Down
Hydroxypropionic acid	Down
Petroselinic acid	Down
Oleic acid	Down
Stearic acid	Down
8-11-14-Eicosatrienoic acid	Down
10-Trans-Heptadecenoic acid	Down
10Z-Heptadecenoic acid	Down
Linoleic acid	Down
Linoelaidic acid	Down
Anserine	Down
Alpha-Linolenic acid	Down
Gamma-Linolenic acid	Down
2-Hydroxy-3-methylbutyric acid	Down
Nonadeca-10Z-enoic acid	Down
Trimethylamine N-oxide	Down
10-13_Nonadecadienoic acid	Down
3-Indolepropionic acid	Down